IOP Conf. Series: Materials Science and Engineering **145** (2016) 052006 doi:10.1088/1757-899X/145/5/052006

Research regarding wires elastic deformations influence on joints positioning of a wire-driven robotic arm

C Ciofu[1], **G Stan**[2]
[1, 2] Department of Industrial Engineering, Vasile Alecsandri University of Bacau, 157 Calea Marasesti Street, Bacau 600115, Romania

E-mail: blgcatalina@yahoo.com

Abstract. In this paper, we present the influence of driving wires deformation on positioning precision of joints from an elephant's trunk robotic arm. Robotic arms driven by wires have the joint accuracy largely depending on wires rigidity. The joint moment of resistance causes elastic deformation of wires and it is determined by: manipulated object load, weight loads previous to the analyzed joint and inherent resistance moment of joint. Static load analysis emphasizes the particular wires elastic deformation of each driven joint from an elephant's trunk robotic arm with five degrees of freedom. We consider the case of a constant manipulated load. Errors from each driving system of joints are not part of the closed loop system. Thus, precision positioning depends on wires elastic deformation which is about microns and causes angle deviation of joints about tens of minutes of sexagesimal degrees. The closer the joints to base arm the smaller positioning precision of joint. The obtained results are necessary for further compensation made by electronic corrections in the programming algorithm of the elephant's trunk robotic arm to improve accuracy.

1. Introducere

Structures of robotic arms with serial connected joints and wire-driven mechanism are similar to elephant's trunk. At the moment, there is a challenge for designers to achieve accuracy with wire-driven robotic arms. These types of robotic structures enable flexible and spatial positioning in confined spaces increasingly necessary in applications from industrial and medical fields.

The number of applications which require the use of elephant's trunk robotic arms is steadily growing, thus, more and more actuation systems and positioning control methods are developed [1]. For instance, robotic fingers, used for gripping different sizes and shapes of objects, are defined by flexible positioning precision and positioning velocity and the optimization of precision positioning is based on structure dynamics [2].

Also, mechanisms driven by actuators placed at the base arm and with actuating wires operating through structure interior are developed for obtaining a minimized diameter of the robotic arm highly required in minimally invasive procedures from medical field [3, 4]. These types of robotic arms have the actuating wires placed outside the closed loop system and an indirect position measurement system. Obtaining accuracy of robotic arms with serial structure and flexible spatial positioning is a concern for many research teams which have made different studies on errors sources and identification methods of errors sources [5-7].

Sources identification of joints positioning errors from the elephant's trunk robotic arm entail an analysis of dynamic behavior for each wire used on actuating of joints. Wires rigidity and resistance

moments of each joint define the dynamic behavior of wires. There are three factors which increase elastic deformation of wires such as: the manipulated object load; the weight loads previously to the analyzed joint; and the inherent resistance moment of joint.

2. Influence analysis of joint resistance moment on precision positioning

The weight loads prior to the analyzed joint are modifying the length to their acting point depending on rotational angle of each joint. The manipulated objects are of different mass values and produce different moments according to the length to their acting point and rotation of each joint respectively. The inherent resistance moment of joint depends on the variation of previously mentioned parameters.

The kinematic structure of elephant's trunk robotic arm with 5 degrees of freedom (DOF) is presented in figure 1. Each joint i=1,...5 is holding several loads such as: weight G_i; variable manipulated object weight G_{mo} and an inherent resistance moment of joint $M_{rp,i}$.

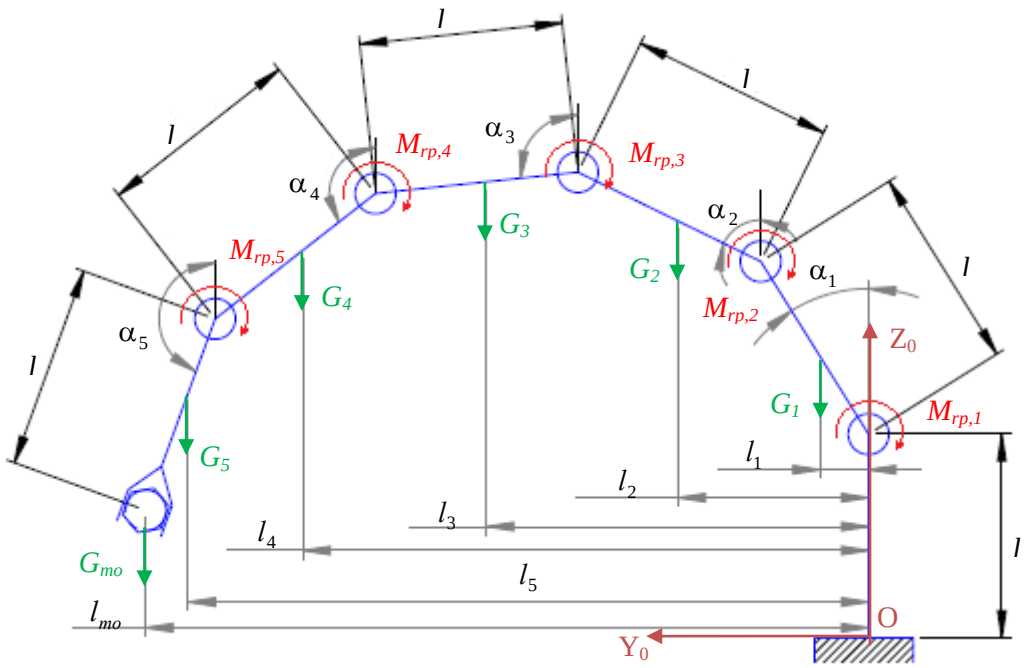

Figure 1. Kinematic structure of the elephant's trunk robotic arm and the loads.

Moments of resistance $M_{r,i}$ are determined using equations (1-5). The length to acting points of moments produced by the weights G_i depend on rotation of the analyzed joint i as denoted by equations (6-7).

$$M_{r,1} = M_{rp,1} + \sum_{i=1}^{5}(G_i \cdot l_i) + G_{mo} \cdot l_{mo} \quad (1)$$

$$M_{r,2} = M_{rp,2} + \sum_{i=2}^{5}(G_i \cdot l_i) + G_{mo} \cdot l_{mo} \quad (2)$$

$$M_{r,3} = M_{rp,3} + \sum_{i=3}^{5}(G_i \cdot l_i) + G_{mo} \cdot l_{mo} \quad (3)$$

$$M_{r,4} = M_{rp,4} + \sum_{i=4}^{5}(G_i \cdot l_i) + G_{mo} \cdot l_{mo} \quad (4)$$

$$M_{r,5} = M_{rp,5} + G_5 \cdot l_5 + G_{mo} \cdot l_{mo} \quad (5)$$

$$l_i = \sum_{k=1}^{i} l \cdot \left(\sin \alpha_{k-1} + \frac{\sin \alpha_k}{2} \right),\ l_{mo} = \sum_{i=1}^{5} l \cdot \sin \alpha_i \tag{6}$$

Parameter α_i denotes the rotational angle of i^{th} joint to axis Z_0 from the base arm, figure 1, and is given by equation (7).

$$\alpha_i = \sum_{k=1}^{i} \theta_k \tag{7}$$

The tension force T_i is acting on the active wire (actuating wire) which rotates joint i and it is determined using equation (8), where r_i denotes i^{th} joints radius.

$$T_i = M_{r,i} / r_i \tag{8}$$

Elastic deformation of the active wire is denoted by Δl_i as in equation (9). The active wire rotates the joint in a direction as indicated in figure 2 and, thus, appears the inherent moment of resistance $M_{rp,i}$ which acts in the opposite direction of joint rotation. The joint is rotating around axis X when the wires fixed at the top end by diametrically opposed pins are pulled by an actuated pulley.

$$\Delta l_i = T_i \cdot L_i / (E \cdot A_s) \tag{9}$$

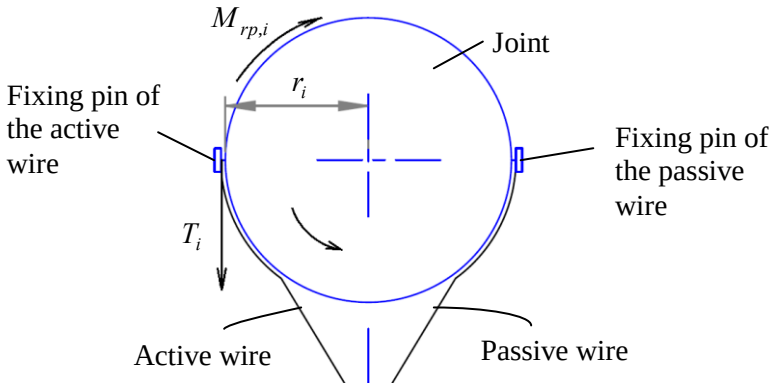

Figure 2. Inherent resistance moment of joint *i*.

In equation (9) we used parameter L_i which denotes the initial length of active wire on which acts the tension force T_i. Using equations (8, 9) we obtain the elastic deformation Δl_i of active wire i depending on resistance moment as described by equation (10).

$$\Delta l_i = M_{r,i} \cdot L_i / (E \cdot A_s \cdot r_i) \tag{10}$$

The elastic deformations of wires employ positioning deviations of joints because the pulley mechanism with wires is not part of the closed loop system. Angle deviation $\Delta\theta_i$ of joint i vary depending on resistance moments of joint $M_{r,i}$ as described by equation (11).

$$\Delta\theta_i = 180 \cdot \Delta l_i / (\pi \cdot r_i) = 180 \cdot M_{r,i} \cdot L_i / (E \cdot A_s \cdot r_i^2 \cdot \pi) \tag{11}$$

From equation (11) we find an inversely proportional relationship between angle deviation $\Delta\theta_i$ and joint radius r_i. The value of structural parameter r_i is given depending on the robotic arm thickness. Most of the industrial applications and, especially, those from medical field impose a fix

value of joint diameter, and of radius respectively, which should be as small as possible. Therefore, increasing joint diameter to obtain a smaller angle deviation is not the convenient solution.

3. Variation of joint positioning precision

According to the literature positioning errors of distal end from elephant's trunk robotic arms have different sources either geometrical or nongeometrical. Moments of resistance are one of the increasing factors of nongeometric errors and cause elastic deformation of the actuating wires. The influence of elastic deformation Δl_i on the variation of joint precision positioning $\Delta\theta_i$ is determined using equations from section 2. For the analysis we consider that each joint is rotating in the same direction as the previous joint to find maximum values of angle deviation.

Equations (1-6, 10) denote that elastic deformation variation of wires used for actuating the robotic arm joints is determined depending on structural and functional parameters. Elephant's trunk robotic arm with 5 DOF has the following features: length between joints l = 50 *mm*; length of 1st joint actuating wire L_1=150 *m*, length of 2nd joint actuating wire L_2=200 *mm*, length of 3rd joint actuating wire L_3=250 *mm*, length of 4th joint actuating wire L_4=300 *mm*, length of 5th joint actuating wire L_5=350 *mm*; joint weight G_i=1 *N*; a constant weight of manipulated object G_{mo}=2 *N*; wire cross sectional area A_s=0,114 mm^2; joint rotation θ_i=±23°; joint radius r_i=16 *mm*.

The elastic modulus, *E*, is experimentally determined for the wire made of nylon-coated stainless steel which actuates the robotic arm joints. Figure 3 denotes stress-strain curve for the nylon-coated stainless steel wire of 75 *mm* length.

In figure 3 we noted: the curve between origin and point A as wire proportionality limit σ_p=600·10^5 N/m^2; point B as wire elasticity limit σ_e=958·10^5 N/m^2; and point C as wire yield point σ_y=1473·10^5 N/m^2. Using Hooke law we obtain elastic modulus of the wire made of nylon-coated stainless steel, E=252523·10^6 N/m^2.

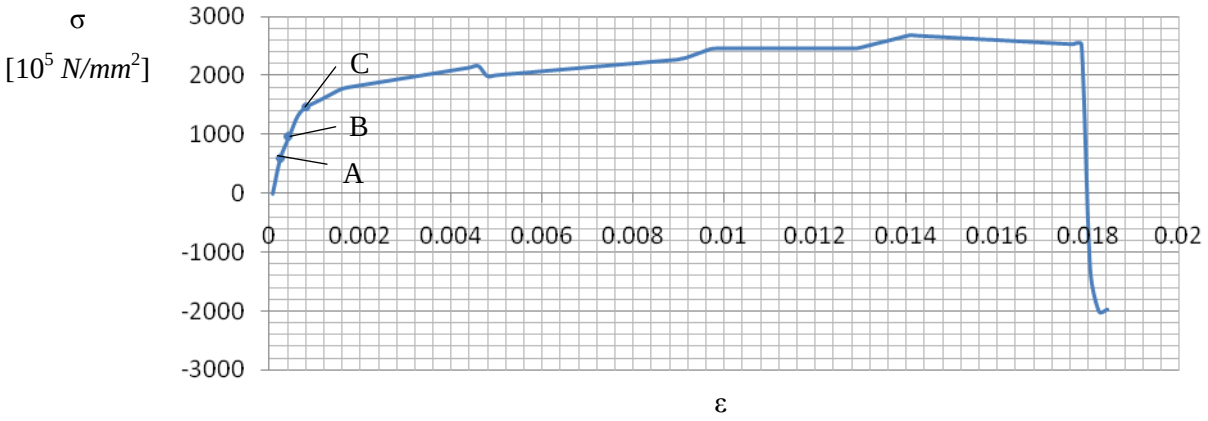

Figure 3. Stress-strain curve for the nylon-coated stainless steel wire.

Elastic deformation of the actuating wires Δl_i varies depending on the loading of resistance moments as represented in the plot from figure 4. Elastic deformation variation is given by the variability of several specific parameters as: resistance moments $M_{r,i}$, length of wires L_i and rotation of joints θ_i. Thus, the maximum elastic deformations obtained reach maximum values: 294 μm for the 1st joint actuating wire, 331 μm for the 2nd joint actuating wire, 294 μm for the 3rd joint actuating wire, 208 μm for the 4th joint actuating wire, 104 μm for the 5th joint actuating wire.

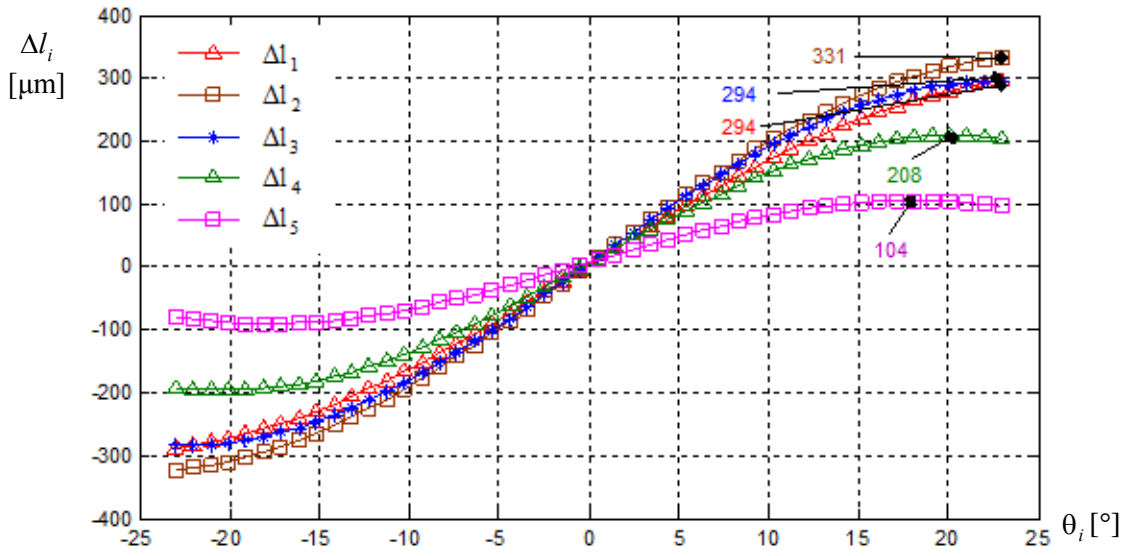

Figure 4. Elastic deformation variation of each driving wire.

The angle deviation denotes precision positioning of joint, $\Delta\theta_i$, which varies and depends directly on the angle values θ_i and on the manipulated object weight G_{mo}. The closed positioning loop of each joint isn't automatically compensating these deviations because the position transducer doesn't have signals for this adjustment function. The obtained variation of positioning precision is highlighted for each joint in figure 5.

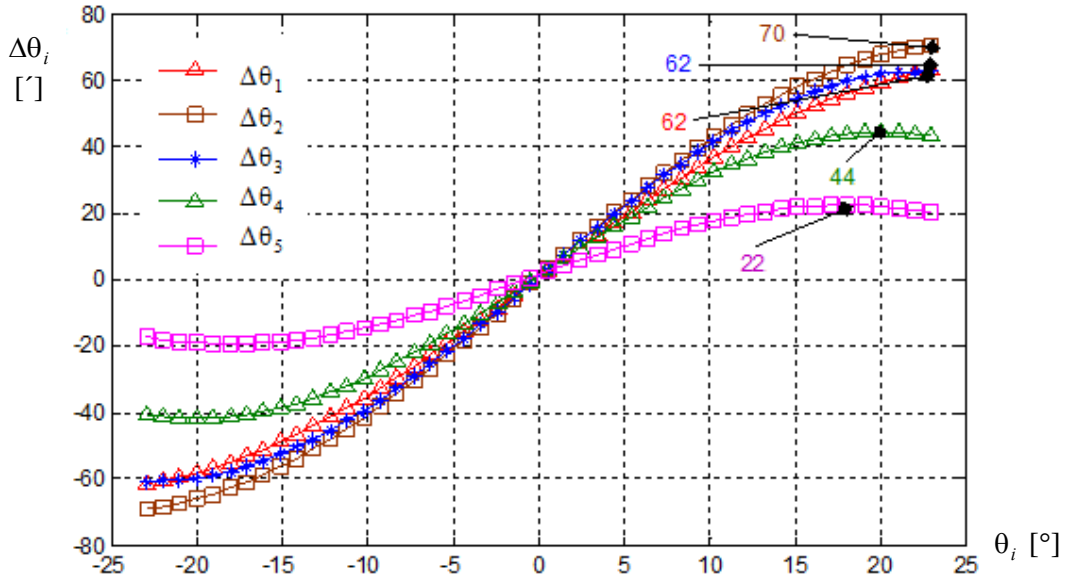

Figure 5. Precision positioning variation of each joint.

Elastic deformation of wires affects the kinematic parameter θ_i with a value given by the angle deviation $\Delta\theta_i$ which varies depending on joints rotation and reaches maximum values: 62´at 1st joint angle deviation; 70´ at 2nd joint angle deviation; 62´ at 3rd joint angle deviation; 44´ at 4th joint angle deviation; 22´ at 5th joint angle deviation.

The two diagrams from figures 4 and 5 we find that elastic deformation of active wire and angle deviation of the 1st joint increase simultaneously with joint rotation. This growing of the two parameters (wire elastic deformation and angle deviation) is noticed at the 2nd and the 3rd joint too. However, elastic deformation values of the active wire and, of angle deviation implicitly, are higher at the 2nd joint than at the 3rd joint ($\Delta l_2 > \Delta l_3, \Delta\theta_2 > \Delta\theta_3$). Elastic deformations of 3rd joint actuating wire are higher than of the 1st joint, and the same dependency is found at angle deviations ($\Delta l_3 > \Delta l_1$, $\Delta\theta_3 > \Delta\theta_1$). This effect is due to the increase of driving wire length from first joint to the last one ($L_1 < L_2 < L_3 < L_4 < L_5$) while the resistance moments of each joint decrease from first to the last one ($M_{r,1} > M_{r,2} > M_{r,3} > M_{r,4} > M_{r,5}$).

Elastic deformations of the 4th and 5th joint actuating wire, Δl_4 and Δl_5 respectively, vary until reaches maximum values at a rotation of 20° and 18° from the origin position of joint respectively. These variations equate with the differences between actuating wires length and resistance moments of each joint from the particular structure of elephant's trunk robotic arm.

4. Conclusion

Elastic deformations of actuating wires from the elephant's trunk robotic arm vary because of the structure loads. The minimum values of positioning precision for the first three joints are obtained solely when each joint reaches the maximum rotation. For the next two joints, the 4th and the 5th, we obtained minimum values of precision positioning when each joint reaches the rotation of 20° and 18° from the origin position of joint respectively. Also, the analysis emphasize that joints closer to base arm have resistance moment much higher than those closer to distal end. Thus, precision positioning of joints vary depending on resistance moments from each joint which employs adequate dimensioning of the elephant's trunk robotic arm.

The moments of resistance estimated in the structural loads analysis of elephant's trunk robotic arm are necessary for a convenient dimensioning of actuators torque to drive the joints. Thus, for the considered robotic arm it is necessary further dimensioning of entire machine system elements.

Robotic arms driven by wires through inner structure have the transmission system outside of the closed loop command system. Thereby, elastic deformations of the actuating wires cause position deviations of joints and, if not compensated, employ positioning errors. These predictable deviations of joints position can be compensated with electronic corrections applied in the programming algorithm of robotic arm to increase positioning precision.

5. References

[1] Walker I D, 2013, Continuous Backbone "Continuum" Robot Manipulators, *ISRN Robotics*.
[2] Dehghani M and Moosavian S A A, 2014, Dynamics Modeling of a Continuum Robotic Arm with a Contact Point in Planar Grasp, *Journal of Robotics*.
[3] Lei M-C and Ruxu D, 2011, Geometry Modeling and Simulation of the Wire-Driven Bending Section of a Flexible Ureteroscope, *Proc. of the World Congress on Eng. and Comp. Sci.* **2**.
[4] Ho M, Ananthanarayanan A, Ehrlich L, Gullapalli R, Simard J M, Gupta S K and Desai J P, 2010, Towards a Minimally Invasive Neurosurgical Intracranial Robot, *IEEE ICRA - Full Day Workshop on S. W. and C.: Continuum and Serp. Rob. for Min. Inv. Surg.*, 27-29.
[5] He B, Wan Z, Li Q, Xie H and Shen R, 2013, An Analytic Method for the Kinematics and Dynamics of a Multiple-Backbone Continuum Robot, *Int. J. of Adv. Robotic Sys.* **10** (84).
[6] Cowan L S and Walker I D, 2012, The Importance of Continuous and Discrete Elements in Continuum Robots, *Interanational Journal of Advanced Robotic Systems* **10** (165).
[7] Trevisani A, 2013, Planning of Dynamically Feasible Trajectories for Translational, Planar and Underconstrained Cable-Driven Robots, *J. Syst. Sci. Complex* **26**.